Title

Low-dose irradiation promotes tissue revascularization through VEGF release from mast cells and MMP-9–mediated progenitor cell mobilization

Journal

Journal of Experimental Medicine, 202(6)

ISSN

0022-1007

Authors

Heissig, Beate
Rafii, Shahin
Akiyama, Haruyo
et al.

Publication Date

2005-09-19

DOI

10.1084/jem.20050959

Peer reviewed

Low-dose irradiation promotes tissue revascularization through VEGF release from mast cells and MMP-9–mediated progenitor cell mobilization

Beate Heissig,[1,2] Shahin Rafii,[3] Haruyo Akiyama,[1] Yuichi Ohki,[1] Yayoi Sato,[1] Tejada Rafael,[3] Zhenping Zhu,[4] Daniel J. Hicklin,[4] Ko Okumura,[2] Hideoki Ogawa,[2] Zena Werb,[5] and Koichi Hattori[1,2]

[1]Institute of Medical Science, University of Tokyo, Tokyo, 108-8639, Japan
[2]Atopy (Allergy) Research Center, Juntendo University School of Medicine, Tokyo, 113-8421, Japan
[3]Department of Hematology-Oncology Cornell University Medical College, New York, NY 10021
[4]ImClone Systems, New York, NY 10014
[5]Department of Anatomy, University of California, San Francisco, CA 94143

Mast cells accumulate in tissues undergoing angiogenesis during tumor growth, wound healing, and tissue repair. Mast cells can secrete angiogenic factors such as vascular endothelial growth factor (VEGF). Ionizing irradiation has also been shown to have angiogenic potential in malignant and nonmalignant diseases. We observed that low-dose irradiation fosters mast cell–dependent vascular regeneration in a limb ischemia model. Irradiation promoted VEGF production by mast cells in a matrix metalloproteinase-9 (MMP-9)–dependent manner. Irradiation, through MMP-9 up-regulated by VEGF in stromal and endothelial cells, induced the release of Kit-ligand (KitL). Irradiation-induced VEGF promoted migration of mast cells from the bone marrow to the ischemic site. Irradiation-mediated release of KitL and VEGF was impaired in MMP-9–deficient mice, resulting in a reduced number of tissue mast cells and delayed vessel formation in the ischemic limb. Irradiation-induced vasculogenesis was abrogated in mice deficient in mast cells (steel mutant, Sl/Sl^d mice) and in mice in which the VEGF pathway was blocked. Irradiation did not induce progenitor mobilization in Sl/Sl^d mice. We conclude that increased recruitment and activation of mast cells following irradiation alters the ischemic microenvironment and promotes vascular regeneration in an ischemia model. These data show a novel mechanism of neovascularization and suggest that low-dose irradiation may be used for therapeutic angiogenesis to augment vasculogenesis in ischemic tissues.

CORRESPONDENCE
Koichi Hattori:
hattoriko@yahoo.com

Abbreviations used: BMNC, BM mononuclear cell; CEP, circulating endothelial progenitor; CFU-C, CFU cell; EC, endothelial cell; eNOS, endothelial nitric oxide synthase; HL, hind limb; IR, irradiation; KitL, Kit-ligand; MCP, monocyte chemotactic protein; MMP, matrix metalloproteinase; MPI, matrix metalloproteinase inhibitor; NO, nitric oxide; PlGF, placental growth factor; rVEGF, recombinant vascular endothelial growth factor; SDF, stromal cell–derived factor; SMA, smooth muscle actin; SMC, smooth muscle cell; TBI, total body irradiation; TGF, transforming growth factor; VEGF, vascular endothelial growth factor; VEGFR, vascular endothelial growth factor receptor; vWF, von Willebrand factor.

Blood vessels form as a result of vasculogenesis from circulating endothelial progenitors (CEPs), angiogenesis, and arteriogenesis through endothelial sprouting from pre-existing vessels. Placental growth factor (PlGF) and vascular endothelial growth factor (VEGF) not only support transient (1) and permanent revascularization of ischemic tissue (2) but also promote mobilization of hematopoietic and/or endothelial progenitor cells (3, 4). They signal through a family of closely related receptor tyrosine kinases consisting of VEGF receptor 1 (VEGFR-1 or Flt-1), VEGFR-2 (Flk-1), and VEGFR-3 (Flt-3). Mast cells also play a role in the formation of new blood vessels. They originate from pluripotent progenitor cells in BM and circulate in small numbers as committed progenitors. Mast cell precursors produce the matrix metalloproteinase (MMP)-9/gelatinase B, which may be essential for mast cell migration into tissues (5). The presence of mast cells in tissues depends on the action of their transmembrane tyrosine kinase receptor, c-kit, and its ligand, kit-ligand (KitL, mast cell growth factor), which is expressed on fibroblasts and stromal cells, from where it can be released.

Ionizing irradiation (IR) has been shown to have angiogenic potential in malignant and nonmalignant diseases (6–8). Although VEGF is an important regulator of vasculogenesis/angiogenesis triggered by IR, hypoxia, and growth

The online version of this article contains supplemental material.

factors, the source and processes supplying VEGF are not well studied. Moreover, the molecular basis of IR-induced angiogenesis is poorly understood. Endothelial cell (EC) viability is not affected at doses of up to 10 Gy, and VEGF has a radioprotective effect on ECs, correlating with the up-regulation of VEGFR-2 in irradiated ECs (9). Up-regulation of IR-induced PlGF in tumor cells causes increased microvessel density in xenografts (10). Prevention of IR-induced angiogenic responses therefore provides an important strategy to prevent tumor recurrence (11). On the other hand, low-dose IR accelerates wound healing and improves neovascularization by promoting EC proliferation (12).

We have investigated the mechanism regulating IR-induced vasculogenesis/angiogenesis in a MMP-9–deficient (MMP-$9^{-/-}$) mouse model. MMPs are involved in many aspects of organ regeneration and angiogenesis by promoting the release of extracellular matrix–bound or cytokines or angiogenesis-modulating extracellular matrix fragments, thereby regulating angiogenesis (13). We demonstrate that MMP-9 plays an important role in stem cell mobilization from the BM niche (4, 14). We now provide evidence that IR-induced vasculogenesis depends in part on MMP-9–mediated release of VEGF from mast cells. Using mast cell–deficient mice or blockade of the VEGF signaling pathway, we demonstrate that KitL and VEGF, when released after IR, not only promote progenitor mobilization but more importantly are potent chemoattractants for mast cells, which serve as a major source of VEGF at the ischemic site.

RESULTS

Impaired BM recovery and progenitor mobilization after irradiation in MMP-9–deficient mice

CEPs contribute to vessel formation at the ischemic site (15). We initially asked whether IR releases hematopoietic progen-

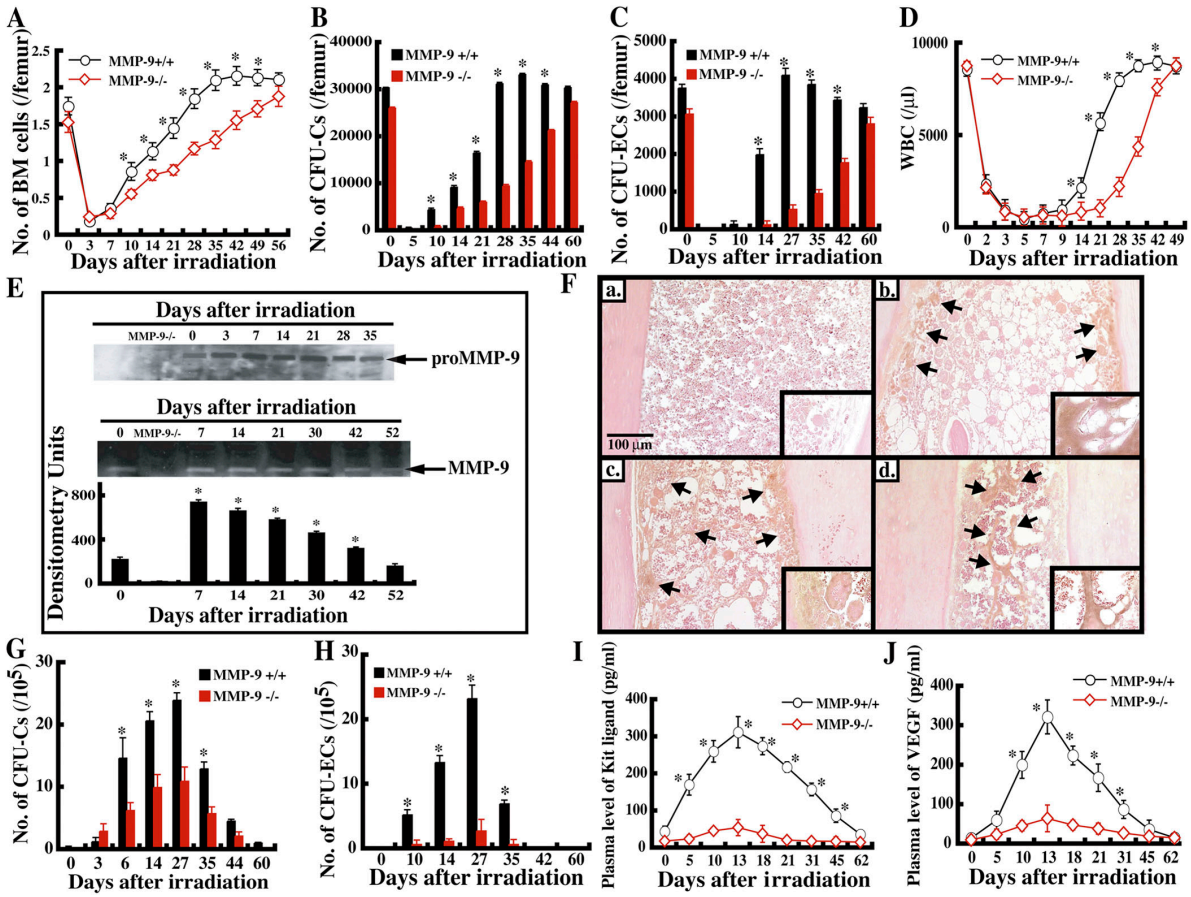

Figure 1. Irradiation-induced BM regeneration and progenitor mobilization are MMP-9–dependent and coincide with an increase in angiogenic factors. MMP-$9^{+/+}$ and MMP-$9^{-/-}$ mice were irradiated with 6.5 Gy. (A) BM cell number (n = 8/group), (B) CFU-Cs (n = 3/group), and (C) CFU-ECs (n = 6/group) were assessed in BM cells following IR (two separate experiments). (D) White blood cell counts (n = 30/group). (E, top) BM cell lysates were assayed via Western blot analysis. (bottom) BM cells obtained after IR were cultured overnight in serum-free medium. BM supernatants were assayed for active MMP-9 via zymography (n = 2; representative experiment shown). Zymographic blot and densitometric quantification are shown. (F) Immunohistochemistry of BM sections before (a) and after IR (b–d) for MMP-9 (brown staining, arrows) in MMP-$9^{+/+}$ and MMP-$9^{-/-}$ mice (original magnification, ×100; insert, ×200). Number of (G) CFU-Cs and (H) CFU-ECs was determined in peripheral blood of irradiated mice. (I, J) Plasma of MMP-$9^{-/-}$ and MMP-$9^{+/+}$ mice was assayed for (I) KitL (n = 5/group) and (J) VEGF (n =5 /group) levels via ELISA. *$P < 0.05$ comparing the MMP-$9^{+/+}$ and MMP-$9^{-/-}$ group. Error bars indicate mean ± SEM.

itors and/or CEP into circulation in an MMP-dependent manner. Both MMP-9–deficient and WT mice tolerated sublethal IR at doses of 1.0, 2.0, 6.5, and 7.5 Gy (unpublished data), and showed no difference in the survival of a lethal IR dose (9.5 Gy). BM hematopoietic recovery after a sublethal dose of 6.5 Gy, as determined by BM cellularity (Fig. 1 A), the hematopoietic colony-forming unit cells (CFU-Cs) (Fig. 1 B), CFU endothelial cell (CFU-EC) recovery (Fig. 1 C), and peripheral blood cell count recovery (Fig. 1 D) was delayed in MMP-9$^{-/-}$ mice compared with controls. These data are in accordance with our previous study in which we showed that MMP-9–mediated KitL release is essential for BM cell recovery, because the delayed BM recovery of MMP-9$^{-/-}$ mice after 5-fluorouracil could be restored by soluble KitL (14).

When WT mice were irradiated with a sublethal dose of 6.5 Gy as total body IR (TBI), MMP-9 expression in supernatants of BM cells increased starting from day 7 until day 21 after IR (Fig. 1 E), while TIMP-1 expression did not change (not depicted). Supernatants of BM cells of unirradiated animals had only small amounts of pro– and active forms of MMP-9. Plasma levels of pro–MMP-9 also increased after IR (Fig. S1 A, available at http://www.jem.org/cgi/content/full/jem.20050959/DC1). Immunoreactive MMP-9 was low in unirradiated mice (Fig. 1 F a) but was highly expressed 6 and 12 d after TBI in close contact with osteoblasts (Fig. 1 F, c and d). By day 30 after IR, MMP-9 staining was found in the central areas of the BM (Fig. 1 F, d). By contrast, MMP-2 expression showed no major change as determined by zymography (Fig. S1 B).

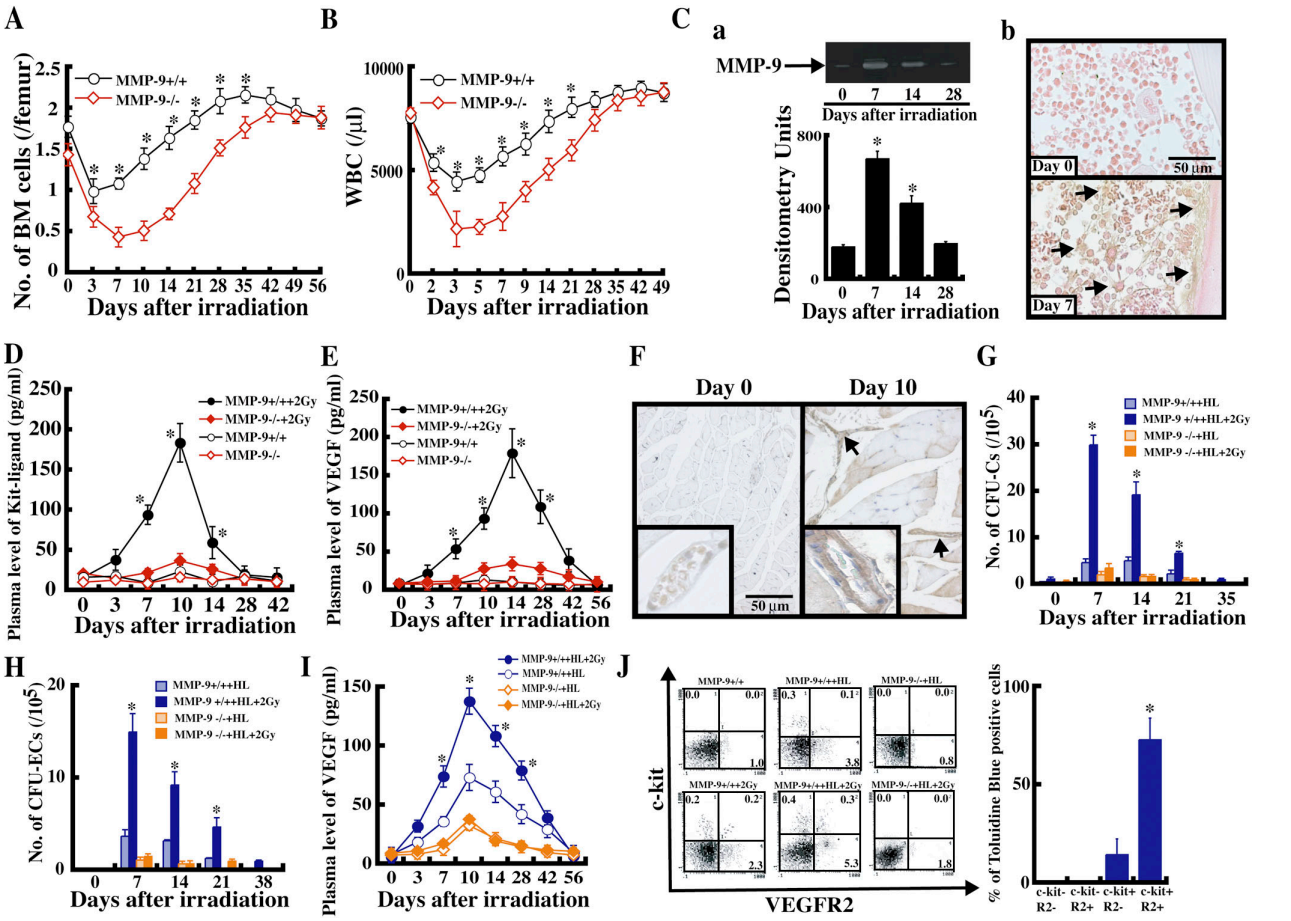

Figure 2. Low-dose irradiation and HL ischemia induce progenitor mobilization. (A–C) MMP-9$^{+/+}$ and MMP-9$^{-/-}$ mice were irradiated with 2 Gy. (A) BM cell number per femur following low-dose IR and (B) white blood cell recovery ($n = 8$) was determined (*$P < 0.05$ comparing MMP-9$^{+/+}$ with MMP-9$^{-/-}$ mice). (C) BM cells were collected after IR and cultured overnight in serum-free conditions. (a) Supernatants were assayed via zymography for active MMP-9 and densitometric quantification (small blot; $n = 3$). (b) Immunohistochemical staining for MMP-9 in BM sections of irradiated animals. Arrows indicate staining for MMP-9. (D, E) Plasma was assayed for KitL (D) and VEGF (E) via ELISA ($n = 2$; *$P < 0.05$ comparing MMP-9$^{+/+}$ group vs. MMP-9$^{+/+}$ + 2 Gy, MMP-9$^{-/-}$, or MMP-9$^{-/-}$ + 2 Gy). (F–J) HL ischemia was induced in MMP-9$^{+/+}$ and MMP-9$^{-/-}$ mice followed by low-dose 2 Gy IR or no IR. (F) Muscle tissue of mice irradiated with 2 Gy was stained for MMP-9 in WT animals on day 0 and day 10. Vessels stained strongly positive for MMP-9 after IR. Arrows indicate positively staining vessels. (G, H) PBMCs were analyzed for the presence of CFU-Cs (G) and CFU-ECs (H) ($n = 6$/group). (I) Plasma VEGF was measured (n = 2; 3–5 mice/group). (J) PBMCs isolated 7 d after IR and HL ischemia was induced were stained for VEGFR-2/Cy2 and c-kit/PE and analyzed via FACS (left). Single- and double-positive VEGFR-2/c-kit PBMCs isolated with a MoFlo cell sorter were stained for Toluidine blue (right). Error bars indicate mean ± SEM.

What is the role of increased MMP-9 activity in the BM endothelium after IR? Under steady-state conditions, the number of capillaries, as a direct measure of BM endothelium, was not different between MMP-$9^{+/+}$ and MMP-$9^{-/-}$ mice. BM vascular recovery following IR was impaired in irradiated MMP-$9^{-/-}$ mice, as estimated by determining the number of capillaries (Fig. S1, C and D). The VEGFR1^{+} (Fig. S1 E) and VEGFR2^{+} cell fractions (Fig. S1 F) were lower in MMP-$9^{-/-}$ mice, and their recovery was delayed.

IR stimulates hematopoietic and endothelial progenitor mobilization

We observed enhanced mobilization of CFU-Cs (Fig. 1 G) and CFU-ECs (Fig. 1 H) into circulation in irradiated WT, but not in MMP-$9^{-/-}$ mice. Which factors govern progenitor mobilization? We recently reported that plasma levels of stromal cell–derived factor 1 (SDF-1 or CXCL12) and KitL are elevated following 5-fluorouracil treatment (stress-hematopoiesis) (4, 14). Here, we show that IR increases stem cell–active mobilization factors, including plasma KitL (Fig. 1 I), VEGF (Fig. 1 J), SDF-1 (Fig. S1 G), and PlGF (Fig. S1 H) in a partly MMP-9–dependent manner.

IR at high doses might have adverse effects. If IR could ultimately be used to improve ischemia-related diseases, low-dose IR could have efficacy in progenitor recovery and growth factor production. Hematopoietic recovery following low-dose IR was delayed in MMP-$9^{-/-}$ as compared with MMP-$9^{+/+}$ mice, as assayed by the number of BM cells per femur (Fig. 2 A). We observed that post-IR–induced leukopenia was attenuated after an IR dose of 2 Gy (Fig. 2 B) in MMP-$9^{-/-}$ mice. Significantly, low-dose IR induced MMP-9 expression in BM cells (Fig. 2 C) and augmented plasma KitL (Fig. 2 D), PlGF (Fig. S2 A, available at http://www.jem.org/cgi/content/full/jem.20050959/DC1), and VEGF levels (Fig. 2 E) in an MMP-9–dependent manner. Moreover, circulating CFU-C and CFU-EC release (Fig. S2 B and C, available at http://www.jem.org/cgi/content/full/jem.20050959/DC1) was increased after low-dose IR in MMP-$9^{+/+}$ but not MMP-$9^{-/-}$ mice.

To test the potential therapeutic pro-angiogenic effect of low-dose IR and its regulation by MMP-9, we chose a mouse model of hind limb (HL) ischemia. Operated MMP-$9^{+/+}$ mice receiving an IR dose of 2 Gy did not show pad necrosis (unpublished data), whereas unirradiated controls showed necrotic changes. In muscle tissue of MMP-$9^{+/+}$ mice, larger vessels stained positive for MMP-9 (Fig. 2 F) after IR (2 Gy). Kidney, lung, and spleen tissue showed no difference in MMP-9 staining before or after IR (unpublished data). HL ischemia increased mobilization of CFU-Cs (Fig. 2 G) and CFU-ECs (Fig. 2 H). However, HL ischemia, in combination with IR, resulted in a profound increase in CFU-Cs (up to 30-fold compared with steady-state values) and CFU-ECs, which coincided with peaks in plasma levels of VEGF (Fig. 2 I), KitL (Fig. S2 D, available at http://www.jem.org/cgi/content/full/jem.20050959/DC1), and PlGF (Fig. S2 E) in MMP-$9^{+/+}$, but not in MMP-$9^{-/-}$ mice. Plasma VEGF, KitL, and PlGF levels rose further (two to threefold) after IR in these mice (Fig. 2 I; and Fig. S2, D and E). Soluble factors known to be involved in ischemic regeneration (16, 17)—such as monocyte chemotactic protein 1 (MCP-1; Fig. S2 F), transforming growth factor β (TGF-β; Fig. S2 G), and basic fibroblast growth factor (unpublished data)—showed slight increases following HL ischemia induction, but were identical in MMP-$9^{+/+}$ and MMP-$9^{-/-}$ mice. Importantly, IR did not further increase the plasma levels of these factors in either group of mice.

To understand which cell types increase after IR, we analyzed peripheral blood mononuclear cells (PBMCs) via FACS (Becton Dickinson) using mAbs against c-kit and VEGFR-2 after IR. No differences were found in the number of VEGFR^{-}/c-kit^{+} cells following HL ischemia or after IR. HL ischemia mobilized VEGFR-2^{+}/c-kit^{-} cells, most likely comprised of ECs (18) in MMP-$9^{+/+}$ mice, but to a lower extent in MMP-$9^{-/-}$ mice (Fig. 2 J). IR further augmented the release of VEGFR-2^{+}/c-kit^{-} cells into circulation in a MMP-9–dependent manner. Importantly, IR increased the VEGFR-2^{+}/c-kit^{+} cell population in MMP-$9^{+/+}$ but not MMP-$9^{-/-}$ mice. Toluidine blue O^{+} cells were the major constituent of the VEGFR-2^{+}/c-kit^{+} fraction (Fig. 2 J).

Low-dose IR stimulates blood vessel formation in ischemic limbs

Revascularization of the ischemic limb was macroscopically delayed in MMP-$9^{-/-}$ mice (unpublished data), with fewer von Willebrand factor (vWF)-positive capillaries, resulting in significantly more necrosis compared with MMP-$9^{+/+}$ mice (Fig. 3, A–C). In addition, the number of vessels covered with smooth muscle cells (SMCs) was higher in HL ischemia–induced MMP-$9^{+/+}$ mice compared with MMP-$9^{-/-}$ animals (Fig. 3 A).

After IR, HL ischemia–induced MMP-$9^{+/+}$ mice showed few signs of necrosis compared with unirradiated controls (Fig. 3, A and B). Muscle tissue from HL ischemia–induced MMP-$9^{-/-}$ mice showed vast areas of necrotic tissue. IR only slightly decreased the necrotic area in these animals. IR under ischemic conditions increased the number of capillaries in MMP-$9^{+/+}$ mice but only slightly in MMP-$9^{-/-}$ mice (Fig. 3 C). Restoration of vascular function as measured by thermography (Fig. 3, A and D) and laser Doppler (Fig. 3, A and E) paralleled the vascular regeneration. Ten days after induction of HL ischemia, laser Doppler analysis revealed decreased blood flow in HL ischemia–induced MMP-$9^{-/-}$ compared with MMP-$9^{+/+}$ mice (Fig. 3 E). IR of HL ischemia–induced MMP-$9^{+/+}$ mice increased both mean temperature (Fig. 3, A and D) and blood flow (Fig. 3, A and E) compared with nonirradiated controls. In contrast, IR of HL ischemia–induced MMP-$9^{-/-}$ mice only slightly improved mean temperature (Fig. 3, A and D) and blood flow (Fig. 3, A and E). Upon histological examination, necrotic area, density of vWF^{+} vessels, and perfusion of irradiated

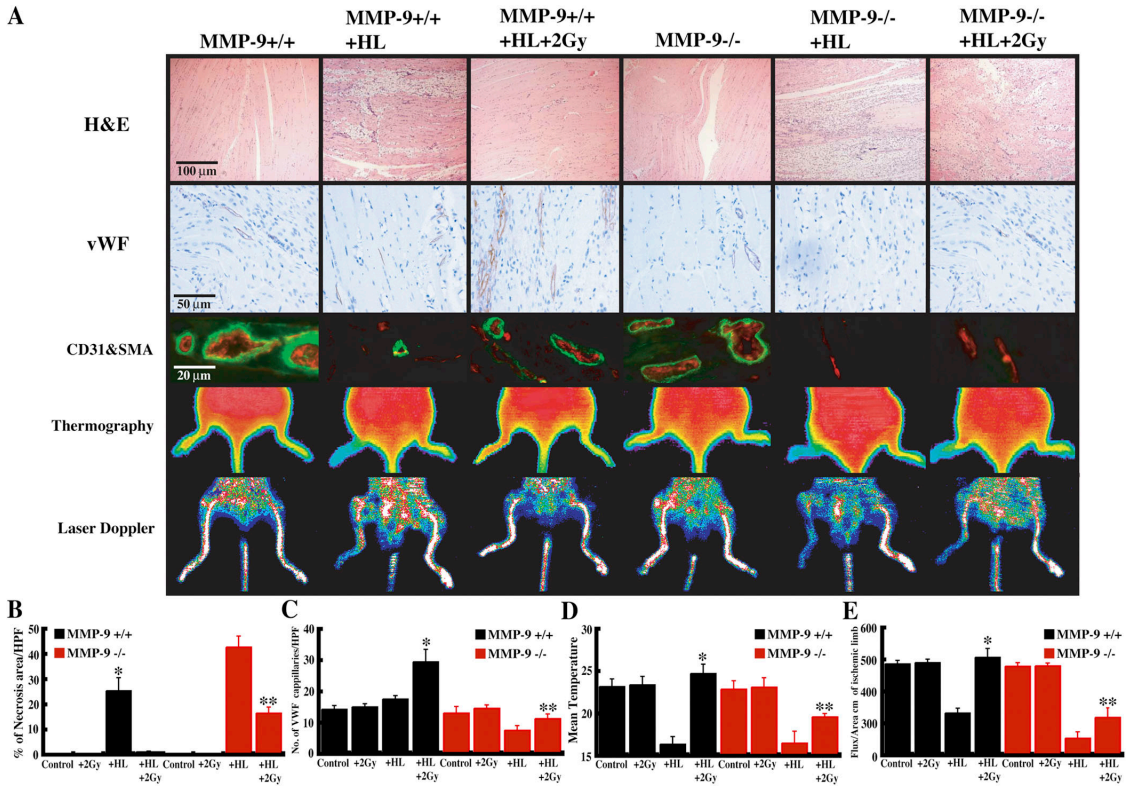

Figure 3. Low-dose IR–mediated revascularization is delayed in MMP-9$^{-/-}$ mice. (A–E) HL ischemia was induced in MMP-9$^{+/+}$ and MMP-9$^{-/-}$ mice. Mice then received a single low-dose TBI (2 Gy) or no IR. (A) Muscle sections from the ischemic limb were stained with hematoxylin-eosin for vWF via immunohistochemistry and with the endothelial marker CD31 (red fluorescence) and SMA (green fluorescence). Mice were analyzed for mean body temperature via thermography 10 d (n = 6/group) and laser Doppler for blood perfusion in the ligated limb 14 d after vessel ligation. (B) Necrosis area of hematoxylin-eosin–stained muscle sections was quantified (n = 3/group). (C) vWF^{+} vessels were counted in muscle sections 7 d following ligation and concomitant IR (n = 3/group). (D) Quantification of the mean temperature 10 d after ligation of the artery and vein (n = 6/group). (E) Blood flux was still low in MMP-9$^{-/-}$ mice on day 14, whereas blood flux had returned to levels seen in nonligated limbs in irradiated MMP-9$^{+/+}$ mice. *P < 0.001 comparing MMP-9$^{+/+}$ mice with HL ischemia without and with IR. **P < 0.05 comparing MMP-9$^{-/-}$ mice with HL ischemia without and with IR or comparing MMP-9$^{+/+}$ and MMP-9$^{-/-}$ with HL ischemia. Error bars indicate mean ± SEM.

animals without induction of ischemia was not different in irradiated compared with unirradiated muscle tissue in MMP-9$^{+/+}$ or MMP-9$^{-/-}$ mice (Fig. 3, B–E). These data suggest that low-dose IR alone does not cause visible changes in the muscle microenvironment, but applied under ischemic conditions stimulates angiogenesis.

IR increases the number of tissue-resident mast cells

The increase in Toluidine blue–positive mast cell–like cells in circulation following IR (Fig. 2 J) led us to hypothesize that IR improves mast cell migration into ischemic tissue. A higher number of mast cells was found in ischemic muscle tissue from MMP-9$^{+/+}$ compared with MMP-9$^{-/-}$ mice (Fig. 4 A, a–d). Mast cells were identified as Toluidine blue– and (unpublished data) mast cell tryptase–positive cells. Using adjacent tissue sections, we detected VEGF mRNA in mast cells via in situ hybridization (Fig. 4 A, e–h), implying that these cells are the major source of VEGF in the tissues after ischemia and IR. Staining of adjacent sections with VEGFR-2 mAb revealed that both mast cells and ECs stained positive for VEGFR-2 (Fig. 4 A, i–l). IR further augmented the number of mast cells in the muscle tissue of MMP-9$^{+/+}$ mice but not MMP-9$^{-/-}$ mice (Fig. 4 A, a–d, m).

Because mice had been exposed to TBI, we determined the number of mast cells in other tissues. The number of Toluidine blue–positive mast cells was higher 14 d after low-dose IR in the skin (Fig. 4 B, a and b) of MMP-9$^{+/+}$ mice, but not MMP-9$^{-/-}$ mice, compared with untreated controls. As a measure of mast cell activation, we determined histamine levels in irradiated and unirradiated WT mice. IR increased plasma histamine levels threefold as compared with unirradiated controls (Fig. S2 H).

Mast cell–mediated VEGF release after low-dose irradiation mediates angiogenesis and is impaired in MMP-9–deficient mice

KitL and VEGF promote mast cell migration (19, 20), and mast cells show baseline MMP-9 activity. We therefore examined whether the decreased number of mast cells in MMP-9$^{-/-}$

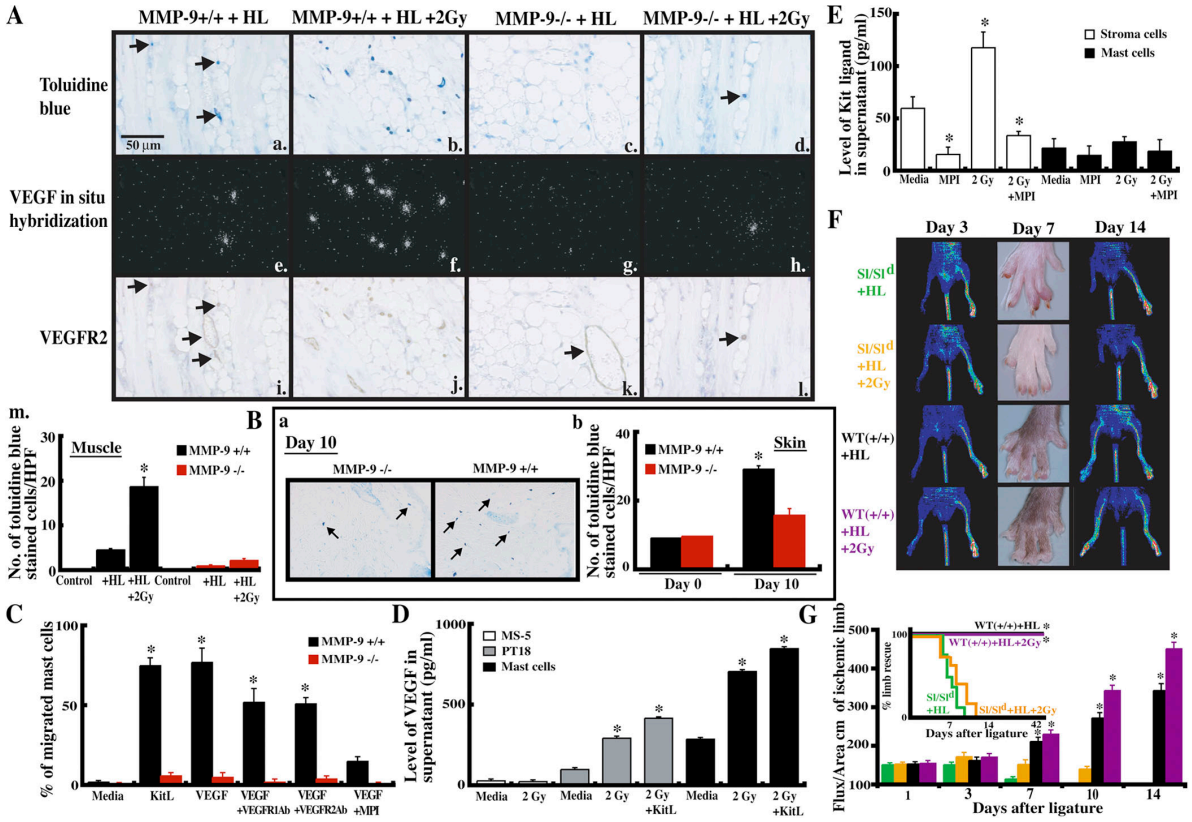

Figure 4. MMP-9–dependent release of VEGF by mast cells and of KitL by stromal cells promotes mast cell migration, a necessary requirement for ischemic regeneration. (A, B) HL ischemia was induced in MMP-9$^{+/+}$ and MMP-9$^{-/-}$ mice, and mice were irradiated with 2 Gy or left unirradiated. Sections of ischemic muscle (A) and skin (B) were stained with Toluidine blue to detect mast cells (a–m). Arrows indicate Toluidine positive mast cells in the ischemic muscle tissue. Adjacent sections of muscle tissue were used for VEGF in situ hybridization (e–h) and immunostaining for VEGFR-2 (i–l). (A, i and l) Arrows indicate the same mast cells stained on adjacent sections for VEGFR2 in ischemic muscle tissue. (A, k) Arrow indicates a VEGFR2 positively stained vessel in ischemic muscle tissue. (B) Arrows indicate Toluidine positively stained mast cells in the muscle tissue. *P < 0.05 (three independent experiments, 3 mice/group; original magnification ×100). (C) BM-derived mast cells from MMP-9$^{+/+}$ and MMP-9$^{-/-}$ mice were plated into transwells. The chemoattractants KitL and VEGF were added to the lower chamber. Data are shown as a percentage of migrated cells (two independent experiments; *P < 0.05 for migration of MMP-9$^{+/+}$ vs. MMP-9$^{-/-}$ cells). (D) Mast cells from MMP-9 WT mice, a mast cell line PT18, and stromal cells (MS-5) were cultured in serum-free medium overnight. Supernatants were assayed for VEGF via ELISA. *P < 0.05 comparing Media with 2 Gy or 2 Gy + KitL groups or 2 Gy group with 2 Gy + KitL group. (E) BM stromal cells and BM-derived mast cells from MMP-9$^{+/+}$ mice were irradiated with 2 Gy in the presence and absence of MPI CGS 27023A. After 24 h in culture, supernatants were assayed for KitL (two independent experiments). *P < 0.05 comparing Media versus MPI or 2 Gy and 2 Gy versus 2 Gy + MPI. (F–G) HL ischemia was induced in SI/SI^d and WBB6F1$^{+/+}$ mice. Groups of mice were irradiated with 2 Gy or were left unirradiated (n = 7). (F) Mice were analyzed via laser Doppler for blood perfusion in the ligated limb (left and right column) or were evaluated macroscopically (middle column). (G) Quantification of blood flow (Flux) after vessel ligation. Insert: percentage of limb rescue. *P < 0.05 comparing WT versus SI/SI^d mice and HL versus HL + 2 Gy group. Error bars indicate mean ± SEM.

mouse tissue was due to a migratory defect of mast cells toward KitL and/or VEGF. In a transwell migration assay, KitL and VEGF induced migration of MMP-9$^{+/+}$ mast cells (Fig. 4 C) but not MMP-9$^{-/-}$ mast cells. VEGF-mediated migration of MMP-9$^{+/+}$ mast cells was partially blocked by neutralizing antibodies against VEGFR-1 or VEGFR-2 but was completely blocked by addition of an MMP inhibitor (MPI CGS 27023A).

PT18 cells (mast cell line) and MMP-9$^{+/+}$ mast cells showed baseline VEGF secretion (Fig. 4 D), which was significantly augmented by 2 Gy IR. Addition of KitL only marginally elevated VEGF levels in supernatant of mast cell cultures. VEGF release depended on the presence of MMP-9, because baseline VEGF secretion from MMP-9$^{-/-}$ mast cells was low, and IR only slightly enhanced VEGF release (Fig. S2 I). The observed differential release of VEGF from mast cells with and without IR was not due to changes in mast cell numbers (unpublished data). The stromal cell line MS-5, on the other hand, produced little VEGF, and VEGF release did not change with IR (Fig. 4 D). Using a more complex BM-derived stromal cell population from MMP-9$^{+/+}$ animals, VEGF secretion did not change before (1961 ± 143 pg/mL) or after IR (2107 ± 150 pg/mL).

Which cell type produces KitL? We show that IR increased KitL release by MS-5 cells in vitro, which could be

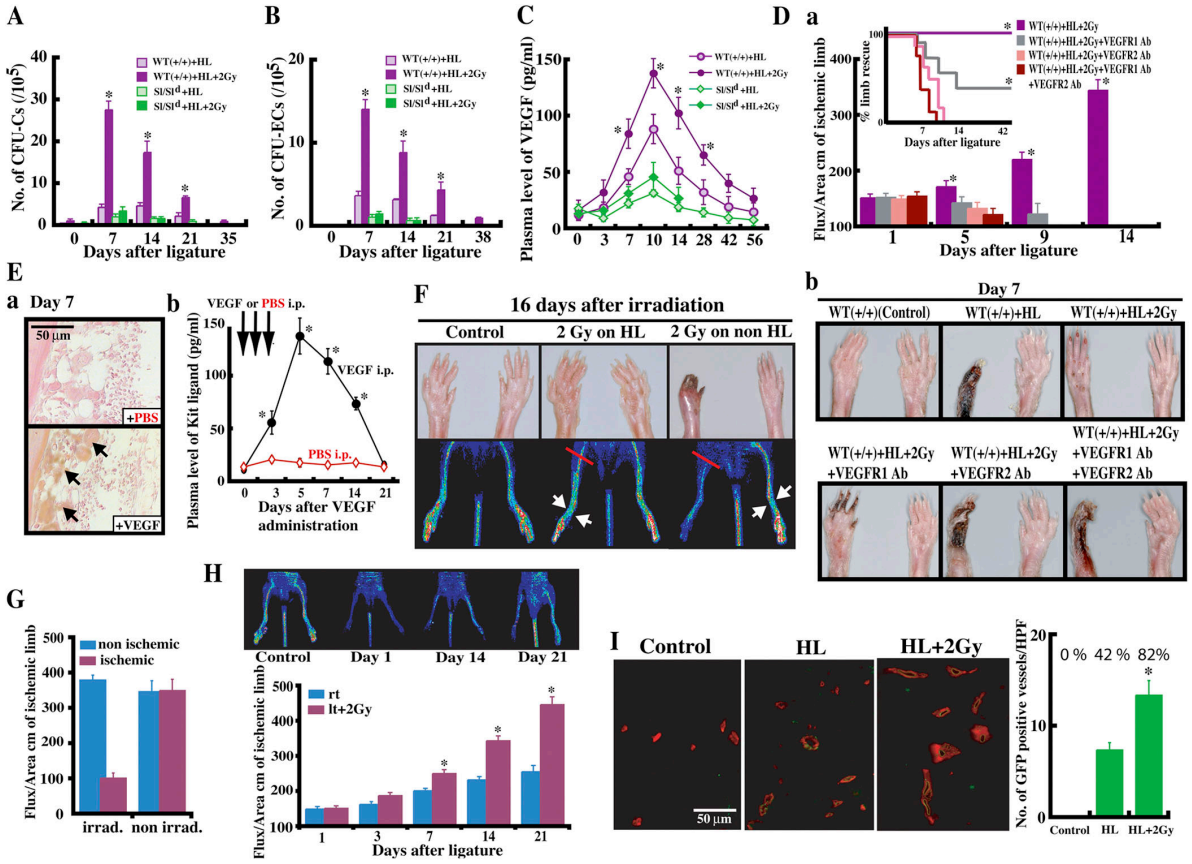

Figure 5. Irradiation-induced angiogenesis is dictated by MMP-9–mediated factor release from mast and stroma cells and incorporation of BM-derived cells. (A–C) HL ischemia was induced in Sl/Sl^d and WBB6F1$^{+/+}$ mice, followed by 2 Gy IR or no IR ($n = 7$). PBMCs were analyzed for the presence of CFU-Cs (A) and CFU-ECs (B). (C) Plasma VEGF was determined ($n = 7$/group). (D) HL ischemia was induced in MMP-9$^{+/+}$ mice followed by 2 Gy IR. Mice were subdivided into groups receiving neutralizing mAbs against VEGFR-1, VEGFR-2 or a combination of both mAbs. (a) Blood flow was determined. Insert: Percentage of mice showing limb rescue after ligation. (b) Macroscopic pictures taken of ischemic and contralateral limb 7 d after ligation (*$P < 0.05$ comparing WT$^{+/+}$ + HL + 2 Gy against VEGFR treatment groups). (E) Administration of rVEGF intraperitoneally augmented MMP-9 staining (arrows indicate MMP-9 staining, brown) in the BM (a) and increased levels for KitL in the plasma of VEGF-treated mice (b) (*$P < 0.05$ comparing VEGF with PBS control). (E, F) MMP-9$^{+/+}$ mice received vessel ligation (red bar) followed by local IR (white arrow) with 2 Gy of the ischemic or the contralateral, nonischemic limb. Arrows indicate that the specified limb received local irradiation, whereas the contralateral limb did not. Macroscopic tissue recovery (on day 16) and blood flow as determined via Doppler analysis on day 10 are shown. (G) From day 1–14, PBMCs from irradiated and unirradiated donor mice were isolated and injected daily into C57BL/6 recipients after HL ischemia surgery. Blood flow was determined on day 7. (H) Bilateral vessel ligation (both limbs) was performed in C57BL/6 mice. Groups of mice received 2 Gy IR unilateral (left, lt). The nonirradiated limb (right, rt) served as a control. Blood flow was quantified via laser Doppler analysis (*$P < 0.05$ comparing bilateral HL vs. bilateral HL + local 2 Gy). (I) C57BL/6 mice were transplanted with GFP$^+$ BMNCs. After cell engraftment, mice underwent vessel ligation with or without 2 Gy IR. (left). Ischemic muscle tissue was stained with SMA-Cy Red. (right). The percentage of GFP$^+$ vessels per total vessels is shown. (A–C) *$P < 0.05$ comparing WT$^{+/+}$ + HL against WT$^{+/+}$ + HL + 2 Gy, Sl/Sl^d + HL, or Sl/Sl^d + HL + 2 Gy. Error bars indicate mean ± SEM.

blocked by a synthetic metalloproteinase inhibitor (Fig. 4 E). In contrast, mast cells only showed baseline secretion of KitL and no change in KitL production after IR. Thus our results indicate cooperation between two cell types in mobilizing mast cells: stromal cells produce KitL, while mast cells produce VEGF in response to IR, and both depend on MMP-9.

To test if IR-induced vasculogenesis/angiogenesis is dependent on mast cells in vivo, mast cell–deficient Sl/Sl^d mice and WBB6F1$^{+/+}$ controls received 2 Gy IR after induction of HL ischemia. Necrosis was macroscopically detectable on day 7 in Sl/Sl^d, but not as profound in the WT mice (Fig. 4 F). By day 14, blood flow recovered in WBB6F1$^{+/+}$ littermates, whereas Sl/Sl^d mice showed complete limb amputation (Fig. 4, F and G). IR accelerated the ischemic recovery in WBB6F1$^{+/+}$ mice, but not in Sl/Sl^d mice (Fig. 4 G). When Sl/Sl^d mice with HL ischemia were treated with IR, all mice died by day 14. These data support the hypothesis that improved angiogenesis after IR is driven by mast cells.

rKitL protects against lethal IR and increases the number of progenitors (21). Mobilization of hematopoietic (Fig. 5 A) and endothelial progenitors (Fig. 5 B) following HL ischemia was similar in WBB6F1$^{+/+}$ and Sl/Sl^d mice; how-

ever, IR-induced progenitor mobilization was completely blocked in Sl/Sl^{d} but not WBB6F1$^{+/+}$ mice, indicating that IR-induced progenitor mobilization depends on the presence of KitL. In confirmation of our data that mast cells are the source of VEGF following HL ischemia and IR, we detected lower VEGF plasma levels in Sl/Sl^{d} mice after HL ischemia as compared with WBB6F1$^{+/+}$ controls (Fig. 5 C); in addition, IR enhanced VEGF plasma levels in WBB6F1$^{+/+}$ but not Sl/Sl^{d} mice.

If VEGF signaling following IR promotes angiogenesis under ischemic conditions, administration of neutralizing antibodies against VEGFR-1 and VEGFR-2 should prevent IR-induced angiogenesis. MMP-9$^{+/+}$ mice received vessel ligation followed by TBI of 2 Gy (Fig. 5 D). Macroscopic examination at day 7 revealed that 2 Gy of IR completely prevented signs of limb necrosis, whereas amputation occurred following HL ischemia (Fig. 5 D, b). The effect of IR in preventing tissue necrosis/amputation was blocked by anti–VEGFR-2 treatment or a combination of anti–VEGFR-1 and anti–VEGFR-2 treatment by day 10, but was only partially inhibited in mice receiving anti–VEGFR-1 by day 14 (Fig. 5 D). Single injections of anti–VEGFR-1 resulted in necrosis but not complete limb amputation.

Administration of rVEGF intraperitoneally caused up-regulation of MMP-9 in BM (Fig. 5 E, a) and increased plasma levels of KitL in treated mice (Fig. 5 E, b). If VEGF promotes mast cell migration into ischemic tissue, blockade of VEGF signaling using VEGFR-1 or VEGFR-2 mAbs should decrease the number of mast cells in the muscle tissue following HL ischemia and/or IR. Indeed, HL ischemia–induced mice treated with VEGFR-2 mAbs or a combination of VEGFR-1 and VEGFR-2 mAbs showed a decreased number of mast cells in the muscle tissue compared with untreated controls (Fig. S2 J). Administration of VEGFR-1 diminished the number of mast cells partially. These data underscore the importance of VEGF signaling in regulating the number of resident mast cells under "stress conditions."

IR promotes angiogenesis by altering the tissue microenvironment

Local low-dose IR rather than TBI would be a more relevant treatment for future clinical applications by reducing systemic side effects. Therefore, C57BL/6 mice received unilateral HL ischemia. Groups of mice were then administered local IR (2 Gy) of the ischemic limb, IR of the contralateral nonischemic limb, or no IR. IR of the contralateral, nonischemic limb controlled for effects due to BM IR. Muscle tissue regeneration was faster in mice when the ischemic limb was irradiated compared with nonirradiated controls (Fig. 5 F). Local IR of the contralateral, nonischemic limb did not result in faster tissue regeneration. Thus, activation of the BM alone was not sufficient to promote angiogenesis. These data implicate that IR of the ischemic tissue, but not of nonischemic tissue, "conditions" the ischemic tissue microenvironment and is critical for IR-induced angiogenesis.

To understand if progenitors mobilized after IR alone could improve vasculogenesis/angiogenesis, PBMCs isolated from irradiated and unirradiated donor mice were transplanted into groups of C57BL/6 recipient mice after HL ischemia surgery. We observed HL ischemic recovery in mice transplanted with PBMCs from unirradiated mice, but not in mice transplanted with PBMCs isolated from 2 Gy irradiated donors (Fig. 5 G). These data implicated that circulating cells induced by IR alone were not sufficient to duplicate the previously observed angiogenesis-promoting effects of IR.

Do BM-derived cells play any role at all in IR-induced angiogenesis under ischemic conditions? When C57BL/6 mice reconstituted with donor GFP-expressing BM cells received HL surgery and 2 Gy IR, BM-derived GFP^{+} cells contributed to vessel formation in muscle tissue of mice that had undergone HL ischemic surgery (Fig. 5 I). These BM-derived cells were covered by smooth muscle actin (SMA)$^{+}$ cells, indicating their incorporation into mature vessels. The highest

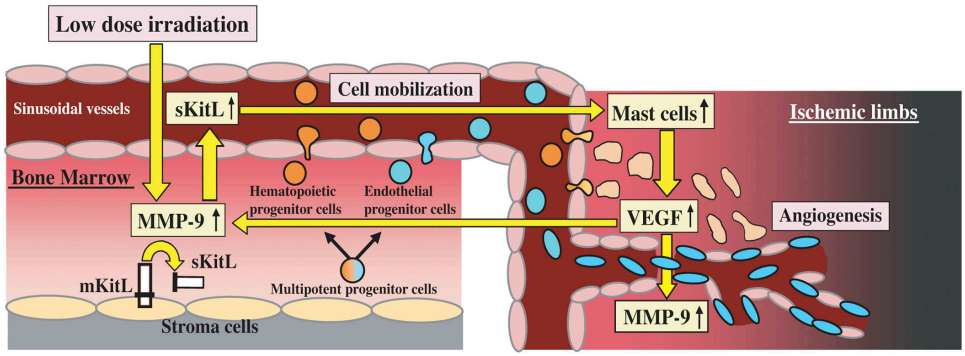

Figure 6. Irradiation modulates neo-angiogenesis within the ischemic microenvironment through VEGF release from mast cells. IR induces up-regulation of MMP-9, resulting in the release of KitL. KitL not only promotes mobilization of progenitors into circulation, which ultimately can be incorporated in ischemic tissue, but also acts as a potent proliferation and migration factor for mast cells. In a partly MMP-9–dependent manner, IR enhances VEGF release from mast cells, which further promote local accumulation of mast cells. VEGF directly can locally support angiogenesis and can further up-regulate MMP-9.

density of donor-derived GFP^+ vessels was found in animals that had received HL ischemic surgery and 2 Gy IR (82%) (Fig. 5 I). Donor-derived GFP^+ cells were undetectable in unirradiated mice without HL ischemia (0%). These data imply that IR applied under ischemic conditions promotes incorporation of BM-derived cells into regenerating vasculature.

To understand whether IR conditions the local ischemic microenvironment to promote mast cell incorporation, we induced bilateral HL ischemia in $WBB6F1^{+/+}$ mice. IR of one leg resulted in faster recovery of blood flow compared with the unirradiated ischemic limb (Fig. 5 H). Increased numbers of mast cells were found in muscle tissue of the irradiated but not the nonirradiated limb (Fig. S2 K, a and b). Plasma levels for VEGF and KitL after bilateral HL ischemia further increased following loco-regional IR (Fig. S2, K, c).

DISCUSSION

We report that low-dose IR promotes neovascularization in the ischemic limb. We provide in vitro and in vivo evidence that mast cells act as a key cellular mediator orchestrating the IR-induced formation of a new vascular network (Fig. 6). IR mediates neovascularization by promoting the release of VEGF from mast cells in a partly MMP-9–dependent manner. VEGF can further up-regulate MMP-9 in the ischemic microenvironment, causing improved mast cell migration. On the other hand, IR-induced KitL increases the number of mast cells in the ischemic tissue and might promote recruitment, incorporation, and differentiation of progenitors into regenerating tissue. The critical importance for mast cells and VEGF in IR-mediated neovascularization under ischemic conditions was underscored by blocking studies using mast cell–deficient Sl/Sl^d mice and blocking Abs against VEGFR-1 and VEGFR-2 to inactivate VEGF signaling.

These data introduce a new mechanism, how IR under ischemic conditions alters the cellular and chemical composition of the ischemic microenvironment. IR promotes tissue regeneration by inducing the expression of genes in mast and stroma cells to further promote incorporation of BM-derived cells, mast cells, pericytes/SMCs, and possibly progenitors to the ischemic side, providing vascular stability and further release of angiogenic factors through the control of proteases. IR has been shown to up-regulate MMP-9 in ECs (22) and to increase the production of nitric oxide (NO) and endothelial nitric oxide synthase (eNOS) (6). NO activates MMP-9 via nitrosylation (23) and improves endothelial and mural cell migration (24). Both NO and eNOS play a critical role in VEGF-induced angiogenesis (25). Mice lacking eNOS show an MMP-9–dependent defect in progenitor cell mobilization and angiogenesis (26). We speculate that the observed IR-induced up-regulation of MMP-9 might involve the NO pathway, but further studies are needed.

Impaired tissue revascularization in MMP-9–deficient mice

BM-derived cells might directly contribute to newly forming vessels or act as bystander cells of the stromal compartment, where they produce cytokines/chemokines (15, 27, 28). Hematopoietic progenitors are mobilized after low-dose IR (29). We show that IR-induced progenitor mobilization is dependent on KitL/mast cells, because no progenitor mobilization was observed in Sl/Sl^d mice. BM-derived GFP^+ cells contributed to vessel formation in ischemic tissues, and IR improved BM cell incorporation in irradiated ischemic tissues. We demonstrated that low-dose IR through VEGF released from mast cells up-regulates MMP-9 in BM stroma and ECs. These data are in accordance with the idea that IR conditions the ischemic microenvironment (mast or stromal cells) to release soluble factors (VEGF or KitL), which can attract circulating cells and promote their tissue incorporation.

Another hint that IR activates the ischemic microenvironment came from the finding that elevated levels of plasma SDF-1, a chemokine produced by stroma cells, was detectable (30). Progenitor mobilization following HL ischemia has been attributed to increased plasma SDF-1 levels (31). Further blocking studies are needed to determine where SDF-1 fits into our pathway of IR-induced angiogenesis.

This report is the first to demonstrate that IR can mobilize CEPs, and that this mobilization is dependent on MMP-9 and KitL, because it did not take place in $MMP\text{-}9^{-/-}$ and Sl/Sl^d mice. We showed reduced angiogenic revascularization in $MMP\text{-}9^{-/-}$ mice on a CD1 background, confirming data by others using $MMP\text{-}9^{-/-}$ mice in C57BL/6 and 129Sv backgrounds (32, 33). Faster ischemic recovery in $MMP\text{-}9^{+/+}$ irradiated mice was associated with improved vessel formation. In contrast, newly formed microvessels in $MMP\text{-}9^{-/-}$ mice showed decreased pericyte coverage and slower ischemic recovery after IR. These data are in accordance with studies showing that VEGF pretreatment of $VEGFR\text{-}1^+$ SMCs activates MMP-9 (34) and that $MMP\text{-}9^{-/-}$ SMCs have decreased cell migration compared with $MMP\text{-}9^{+/+}$ cells in vitro (35).

Mast cell migration and VEGF release from mast cells are defective in $MMP\text{-}9^{-/-}$ mice

The radiosensitivity of white spotting and Sl/Sl^d mice has been attributed to a role for KitL in the proliferation of BM-derived mast cells (36). If IR results in the release of KitL, more $c\text{-}kit^+$ mast cells should be found in irradiated tissue. Indeed, in the recovery phase after IR, concomitant with increased KitL plasma levels, the number of mast cells was higher in muscle tissue of $MMP\text{-}9^{+/+}$ mice compared with $MMP\text{-}9^{-/-}$ mice.

Mast cells migrate into tissues via blood circulation as immature cells and undergo complete maturation in the tissues (37). Murine mast cells migrate toward VEGF (20) and express VEGFR-2 (38). We showed that circulating mast cell–like cells express c-kit and VEGFR-2 and that VEGF-induced mast cell migration was partially blocked using VEGFR mAbs. We demonstrated that $MMP\text{-}9^{-/-}$ mast cells failed to migrate toward KitL and VEGF. These data indicate that VEGF improves mast cell migration by further activating MMPs, because a synthetic MPI blocked this migration. Interestingly, a study by Tanaka et al. showed that MMP-9 promoted the migration of mast cell precursors into tissues (5).

Mast cells contain extracellular matrix–degrading MMPs and constitutively secrete VEGF (39, 40). We demonstrate that VEGF production partly depends on the presence of MMP-9, because baseline VEGF release was low in MMP-$9^{-/-}$ mast cells in vitro. Irradiated MMP-$9^{+/+}$ mast cells secreted more VEGF than unirradiated mast cells, consistent with a study showing that VEGF gene expression was upregulated in irradiated versus unirradiated cells (7). Blocking VEGF signaling using neutralizing mAbs against VEGFR-1 and VEGFR-2 prevented mast cell migration and IR-induced vasculogenesis/angiogenesis. Interestingly, we detected increased levels of histamine in the plasma of IR animals as early as 6 h, indicating that mast cell activation had taken place.

Our data show that mast cells are critical in ischemic recovery and IR-induced angiogenesis: ischemic regeneration was delayed, the number of IR-induced circulating progenitors reduced, and the VEGF plasma levels following IR were significantly lower in mast cell–deficient Sl/Sl^d mice than in unirradiated WT mice. Even though the release of VEGF and KitL depends in part on MMP-9, MMP-$9^{-/-}$ mice do not completely lack these factors and show growth factor elevation to some degree after ischemia and IR. The leakiness in the system might explain why improved tissue vascularization was detectable in MMP-$9^{-/-}$ mice, albeit at lower levels. It is also conceivable that MMP-9–independent angiogenesis-modulating factors are released from mast cells under ischemic conditions, but future studies will be necessary. These data support our current model that VEGF and mast cells, partly under the control of MMP-9, are critical in the angiogenesis-promoting effect of IR. It is conceivable that growth factor–independent IR can modulate the vascular tonus of the distal vasculature (41).

Clinical implications

The results of the present study have important implications for the use of radiotherapy in nonmalignant and malignant diseases. We demonstrated the clinical potential of low-dose IR to induce neovascularization in ischemia-associated diseases. However, potential adverse effects due to the release of KitL and/or activation of mast cells might occur, including mast cell degranulation with increased pruritus, increased melanization of the epidermis, and allergic-like reactions such as urticaria, with or without respiratory symptoms (42). Likewise, long-term studies are needed to rule out negative side effects resulting from local IR. We propose that IR modulates the ischemic and possibly tumor microenvironment via MMP-9–mediated cytokine and angiogenic factor-driven mast cell and progenitor recruitment. We identified mast cells as a major source of VEGF release, which is known to promote tumor-angiogenesis. Tumor growth is controlled by angiogenesis. In cancer patients, the cytotoxic effect of low-dose IR on tumor cells might outweigh the IR-induced proangiogenic effects, resulting in a net tumor mass reduction. On the other hand, our model might shed light into clinical settings in which a tumor returned despite initial killing of tumor cells. Radio-resistant mast cells, whose number could be further increased by IR-induced release of KitL might guide those processes (21).

MATERIALS AND METHODS

Animals

MMP-$9^{+/+}$ and MMP-$9^{-/-}$ mice were used after >10 back crosses to CD1 mice (14). KitL WT (WBB6F$1^{+/+}$) and KitL-deficient (Sl/Sl^d) and C57BL/6 mice were purchased from SLC. Mice expressing GFP under a β-actin promoter were provided by A. Urabe (Juntendo University, Tokyo, Japan). Animal studies had been approved by the Animal Review Board of Juntendo University, Tokyo.

Irradiation in vivo

MMP-$9^{+/+}$ and MMP-$9^{-/-}$ mice were irradiated with 1, 2, 6.5, or 9.5 Gy (Caesium Gy source). Sl/Sl^d and WBB6F$1^{+/+}$ littermates were irradiated with 2 Gy. For local IR (2 Gy), mice were kept in a radio-dense 2-cm-thick lead cage; only the irradiated limb left the cage.

VEGF administration

MMP-$9^{+/+}$ mice received rVEGF 300 ng/mouse/d intraperitoneally.

PBMC transplantation

PBMCs (2×10^6/mouse) from irradiated (2 Gy) and unirradiated C57BL/6 mice (from day 0–16) were injected intravenously into unirradiated HL ischemia–induced mice.

HL model

Unilateral or bilateral ligation of the femoral artery and vein and cutaneous vessels branching from the caudal femoral artery side branch were performed. Groups of MMP-$9^{+/+}$ and MMP-$9^{-/-}$ mice or Sl/Sl^d and WBB6F$1^{+/+}$ littermates were then irradiated with or without 2.0 Gy. Tissue sections from the lower muscles of ischemic limbs were harvested. Thermography of the collateral region was performed using a Lisca PIM II camera (Gambro). A laser Doppler perfusion image analyzer (Moor Instruments) recorded blood flow postoperatively. Blood was collected via retro-orbital bleeding using heparinized capillaries. Plasma samples were stored at −80°C. White blood cell counts were determined. PBMCs were isolated from heparinized blood after centrifugation over Lympholyte-M (Cedarlane).

In vivo blocking experiments

Unilateral HL ischemia–inducing surgery was performed on MMP-$9^{+/+}$, WBB6F$1^{+/+}$, or Sl/Sl^d mice receiving 2 Gy or no IR. Mice were coinjected intraperitoneally with 800 μg anti–mouse VEGFR-1 (MF-1), anti–mouse VEGFR-2 (DC101), or IgG at 2-day intervals starting at day 0 (4).

Histological assessment

Paraffin-embedded sections were deparaffinized and stained with hematoxylin-eosin. Vascular structures within the BM with EC morphology, which contained erythrocytes, were counted as capillaries in hematoxylin-eosin–stained BM. The mean number of capillaries per square millimeter (capillary density) of vWF stained slides was counted. The mean ischemic area per square millimeter (n = 10) of hematoxylin-eosin–stained slides was determined using an image analyzer (Carl Zeiss Vision, Hallbergmoss). Necrotic muscle fibers were identified via morphology, differential eosin staining, and presence of infiltrating cells near degenerating fibers. Paraffin sections of muscle or skin sections were stained with Toluidine blue O, and mast cells were counted under a light microscope.

Deparaffinized BM sections were stained for MMP-9 (7-11C) or a murine Ab against MMP-9 as described (14). Muscle sections were stained with CD31 (BD Biosciences, MEC13.3), vWF (DakoCytomation) or VEGFR-2 (DC101). vWF stained sections were developed with 3′,3′-diaminobenzidine. ECs were identified using rat mAb against mouse CD31 followed by biotin-conjugated Goat anti–rat IgG and Cy3-conjugated streptavidin (Alexa 594, Molecular Probes) staining. SMCs were identified using mouse anti-

human SMA (1A4) followed by biotin-conjugated Goat anti–mouse IgG and FITC-conjugated streptavidin (Alexa 488, Molecular Probes).

In situ hybridization for VEGF

VEGF was detected in muscle sections using a murine-specific probe for VEGF as described previously (43).

In vitro assays

Murine BM cultures. Murine BM cells (10^6 cells) from MMP-$9^{+/+}$ and MMP-$9^{-/-}$ isolated before and after TBI were placed in serum-free medium (X-VIVO-15) overnight. Supernatants were analyzed via Western blotting using murine mAb to MMP-9 as described previously (14).

Murine PBMC isolation. Groups of MMP-$9^{+/+}$ and MMP-$9^{-/-}$ mice were set up in which HL ischemia was followed by 2 Gy IR or no IR. Mice were bled on day 7. PBMCs were labeled with VEGFR-2/Cy2 and c-kit/PE, separated using MoFlo. Cytospins were prepared from the cell fractions, which were stained with Toluidine blue.

PT18 and MS-5 cultures. PT18 cells (5×10^5 cells/mL) and a confluent layer of MS-5 cells were cultured for 48 h in serum-free medium. Cells were irradiated using a dose of 2 Gy or were not irradiated. Supernatants were stored at −20°C.

Murine BM mast cell cultures. BM-derived mast cells were produced by culturing MMP-$9^{+/+}$ and MMP-$9^{-/-}$ BM cells in RPMI 1640 supplemented with 0.075% sodium bicarbonate (Sigma), 1 mM nonessential amino acids (GIBCO BRL), 5.5×10^{-5} M 2-ME (Wako), 1 mM sodium pyruvate (ICN Biomedicals), 10% FBS (GIBCO BRL), and 10% WEHI-3–derived conditioned medium. Mast cells from 3-wk cultures were cultured over night in serum-free medium (Ex Vivo 15). Supernatants were stored at −20°C. 3-wk-old BM mast cell cultures contained >97% c-kit$^+$ cells by FACS and 95% Toluidine blue$^+$ cells.

Mast cell transmigration. Mast cells derived from MMP-$9^{+/+}$ and MMP-$9^{-/-}$ BM cultures were added to 5-μm pore size transwell inserts (Costar). Murine rKitL (100 ng/mL; PeproTech) or rVEGF (200 ng/mL; PeproTech) were added to the lower chamber with/without neutralizing mAbs against murine VEGFR1 (MF-1), VEGFR1 (DC101), the MPI CGS 27023A (1 nM; Novartis), and neutralizing mAbs against KitL (R&D Systems) that were added to both chambers. Transmigrated cells were expressed as the percentage of transmigrated cells.

Hematopoietic progenitor assay. PBMCs (10^5 cells/plate) or BM mononuclear cells (BMNCs) (10^5 cells/plate) were assayed as described previously (14).

Endothelial progenitor assay. PBMCs or BMNCs before and obtained at various time points after IR (2 Gy) were cultured as described previously (14). To determine the EC origin, adherent cells were stained with anti–mouse VEGFR-2 (Avas-12a1, PharMingen), followed by peroxidase-conjugated streptavidin incubation (DakoCytomation), and visualized using an AEC+ Substrate-Chromosome System (DakoCytomation). Cultures were costained using rat monoclonal anti–mouse CD45 (BD Biosciences) to exclude leukocytes, followed by alkaline phosphatase–labeled streptavidin (Vector), and visualized using Nitro blue Tetrazolium Chloride (DakoCytomation). VEGFR-1$^+$ and VEGFR-2$^+$ cells were quantified via FACS using Cy2-labeled mAb to VEGFR-1 (MF-1) and VEGFR-2 (DC101).

Zymography. Supernatants from BM cells from MMP-9 WT mice before and after IR with 6.5 Gy and 2 Gy were cultured overnight in serum-free medium. Supernatants were analyzed as described previously (14).

Immunoassay. In plasma/culture supernatants SDF-1, VEGF, PlGF, KitL, MCP-1, and pro–MMP-9 were measured via ELISA (R&D Systems). TGF-β plasma levels were assayed using a TGF-β ELISA kit (Genzyme Boston). Plasma obtained 20 min after IR was analyzed for histamine via ELISA (ImmunoTECH).

Statistical analysis

Data were analyzed using an unpaired two-tailed Student's *t* test and are expressed as the mean ± SEM. P values less than 0.05 were considered significant.

Online supplemental material

Fig. S1 shows MMP-9 but not MMP-2 expression and plasma levels for SDF-1 and PlGF and BM recovery of VEGFR-1$^+$ and VEGFR-2$^+$ cells following IR with 6.5 Gy. Fig. S2 shows progenitor mobilization after 2 Gy IR and includes data on KitL, PlGF, MCP-1, TGF-β, and histamine release following HL ischemia in combination with 2 Gy IR. Fig. S2 also contains data on VEGF release from mast cells in vitro and data on the number of mast cells in muscle tissues after mice had been treated with neutralizing antibody against VEGFR-1 and VEGFR-2, as well as data on the number of mast cells and the release of VEGF and KitL in mice following bilateral ligation of the femoral artery and vein. Online supplemental material is available at http://www.jem.org/cgi/content/full/jem.20050959/DC1.

We thank Drs. A. Furuhata, N. Tada, and M. Kuhara for their excellent technical assistance and H. Nakauchi for his helpful discussions.

This work was supported by grants from the JSPS (to B. Heissig), the Leukemia and Lymphoma Foundation (to B. Heissig), and the NIH (AG23218 and ES012801 to Z. Werb); Grants-in-Aid for Scientific Research from MEXT (to K. Hattori, B. Heissig); and in part by grants from the Mochida Memorial Foundation (to K. Hattori), AstraZeneka (to K. Hattori), Naito Memorial Foundation (to K. Hattori), Mitsubishi Pharma Research Foundation (to K. Hattori), Mitsukoshi Health and Welfare Foundation (to K. Hattori), Mitsui Life Social Welfare Foundation (to K. Hattori), and Sagawa Foundation (to K. Hattori). Nihon Kohden Co. Ltd. provided thermography analysis.

The authors have no conflicting financial interests.

Submitted: 12 May 2005
Accepted: 28 July 2005

REFERENCES

1. Isner, J.M. 2002. Myocardial gene therapy. *Nature*. 415:234–239.
2. Luttun, A., M. Tjwa, L. Moons, Y. Wu, A. Angelillo-Scherrer, F. Liao, J.A. Nagy, A. Hooper, J. Priller, B. De Klerck, et al. 2002. Revascularization of ischemic tissues by PlGF treatment, and inhibition of tumor angiogenesis, arthritis and atherosclerosis by anti-Flt1. *Nat. Med.* 8:831–840.
3. Hattori, K., S. Dias, B. Heissig, N.R. Hackett, D. Lyden, M. Tateno, D.J. Hicklin, Z. Zhu, L. Witte, R.G. Crystal, et al. 2001. Vascular endothelial growth factor and angiopoietin-1 stimulate postnatal hematopoiesis by recruitment of vasculogenic and hematopoietic stem cells. *J. Exp. Med.* 193:1005–1014.
4. Hattori, K., B. Heissig, Y. Wu, S. Dias, R. Tejada, B. Ferris, D.J. Hicklin, Z. Zhu, P. Bohlen, L. Witte, et al. 2002. Placental growth factor reconstitutes hematopoiesis by recruiting VEGFR1(+) stem cells from bone-marrow microenvironment. *Nat. Med.* 8:841–849.
5. Tanaka, A., K. Arai, Y. Kitamura, and H. Matsuda. 1999. Matrix metalloproteinase-9 production, a newly identified function of mast cell progenitors, is downregulated by c-kit receptor activation. *Blood*. 94: 2390–2395.
6. Sonveaux, P., A. Brouet, X. Havaux, V. Gregoire, C. Dessy, J.L. Balligand, and O. Feron. 2003. Irradiation-induced angiogenesis through the up-regulation of the nitric oxide pathway: implications for tumor radiotherapy. *Cancer Res.* 63:1012–1019.
7. Polytarchou, C., T. Gligoris, D. Kardamakis, E. Kotsaki, and E. Papadimitriou. 2004. X-rays affect the expression of genes involved in angiogenesis. *Anticancer Res.* 24:2941–2945.
8. Moeller, B.J., Y. Cao, C.Y. Li, and M.W. Dewhirst. 2004. Radiation activates HIF-1 to regulate vascular radiosensitivity in tumors: role of reoxygenation, free radicals, and stress granules. *Cancer Cell*. 5:429–441.
9. Kermani, P., G. Leclerc, R. Martel, and J. Fareh. 2001. Effect of ioniz-

ing radiation on thymidine uptake, differentiation, and VEGFR2 receptor expression in endothelial cells: the role of VEGF(165). *Int. J. Radiat. Oncol. Biol. Phys.* 50:213–220.
10. Taylor, A.P., M. Rodriguez, K. Adams, D.M. Goldenberg, and R.D. Blumenthal. 2003. Altered tumor vessel maturation and proliferation in placenta growth factor-producing tumors: potential relationship to post-therapy tumor angiogenesis and recurrence. *Int. J. Cancer.* 105:158–164.
11. Klement, G., S. Baruchel, J. Rak, S. Man, K. Clark, D.J. Hicklin, P. Bohlen, and R.S. Kerbel. 2000. Continuous low-dose therapy with vinblastine and VEGF receptor-2 antibody induces sustained tumor regression without overt toxicity. *J. Clin. Invest.* 105:R15–R24.
12. Schindl, A., G. Heinze, M. Schindl, H. Pernerstorfer-Schon, and L. Schindl. 2002. Systemic effects of low-intensity laser irradiation on skin microcirculation in patients with diabetic microangiopathy. *Microvasc. Res.* 64:240–246.
13. Heissig, B., K. Hattori, M. Friedrich, S. Rafii, and Z. Werb. 2003. Angiogenesis: vascular remodeling of the extracellular matrix involves metalloproteinases. *Curr. Opin. Hematol.* 10:136–141.
14. Heissig, B., K. Hattori, S. Dias, M. Friedrich, B. Ferris, N.R. Hackett, R.G. Crystal, P. Besmer, D. Lyden, M.A. Moore, et al. 2002. Recruitment of stem and progenitor cells from the bone marrow niche requires MMP-9 mediated release of kit-ligand. *Cell.* 109:625–637.
15. Rafii, S., D. Lyden, R. Benezra, K. Hattori, and B. Heissig. 2002. Vascular and haematopoietic stem cells: novel targets for anti-angiogenesis therapy? *Nat. Rev. Cancer.* 2:826–835.
16. Buschmann, I., M. Heil, M. Jost, and W. Schaper. 2003. Influence of inflammatory cytokines on arteriogenesis. *Microcirculation.* 10:371–379.
17. Niiyama, H., H. Kai, T. Yamamoto, T. Shimada, K. Sasaki, T. Murohara, K. Egashira, and T. Imaizumi. 2004. Roles of endogenous monocyte chemoattractant protein-1 in ischemia-induced neovascularization. *J. Am. Coll. Cardiol.* 44:661–666.
18. Shalaby, F., J. Rossant, T.P. Yamaguchi, M. Gertsenstein, X.F. Wu, M.L. Breitman, and A.C. Schuh. 1995. Failure of blood-island formation and vasculogenesis in Flk-1-deficient mice. *Nature.* 376:62–66.
19. Taylor, M.L., J. Dastych, D. Sehgal, M. Sundstrom, G. Nilsson, C. Akin, R.G. Mage, and D.D. Metcalfe. 2001. The Kit-activating mutation D816V enhances stem cell factor–dependent chemotaxis. *Blood.* 98:1195–1199.
20. Gruber, B.L., M.J. Marchese, and R. Kew. 1995. Angiogenic factors stimulate mast-cell migration. *Blood.* 86:2488–2493.
21. Heissig, B., Z. Werb, S. Rafii, and K. Hattori. 2003. Role of c-kit/Kit ligand signaling in regulating vasculogenesis. *Thromb. Haemost.* 90:570–576.
22. Nirmala, C., S.L. Jasti, R. Sawaya, A.P. Kyritsis, S.D. Konduri, F. Ali-Osman, J.S. Rao, and S. Mohanam. 2000. Effects of radiation on the levels of MMP-2, MMP-9 and TIMP-1 during morphogenic glial-endothelial cell interactions. *Int. J. Cancer.* 88:766–771.
23. Gu, Z., M. Kaul, B. Yan, S.J. Kridel, J. Cui, A. Strongin, J.W. Smith, R.C. Liddington, and S.A. Lipton. 2002. S-nitrosylation of matrix metalloproteinases: signaling pathway to neuronal cell death. *Science.* 297:1186–1190.
24. Kashiwagi, S., Y. Izumi, T. Gohongi, Z.N. Demou, L. Xu, P.L. Huang, D.G. Buerk, L.L. Munn, R.K. Jain, and D. Fukumura. 2005. NO mediates mural cell recruitment and vessel morphogenesis in murine melanomas and tissue-engineered blood vessels. *J. Clin. Invest.* 115:1816–1827.
25. Fukumura, D., T. Gohongi, A. Kadambi, Y. Izumi, J. Ang, C.O. Yun, D.G. Buerk, P.L. Huang, and R.K. Jain. 2001. Predominant role of endothelial nitric oxide synthase in vascular endothelial growth factor-induced angiogenesis and vascular permeability. *Proc. Natl. Acad. Sci. USA.* 98:2604–2609.
26. Aicher, A., W. Brenner, M. Zuhayra, C. Badorff, S. Massoudi, B. Assmus, T. Eckey, E. Henze, A.M. Zeiher, and S. Dimmeler. 2003. Assessment of the tissue distribution of transplanted human endothelial progenitor cells by radioactive labeling. *Circulation.* 107:2134–2139.
27. Lyden, D., K. Hattori, S. Dias, C. Costa, P. Blaikie, L. Butros, A. Chadburn, B. Heissig, W. Marks, L. Witte, et al. 2001. Impaired recruitment of bone-marrow-derived endothelial and hematopoietic precursor cells blocks tumor angiogenesis and growth. *Nat. Med.* 7:1194–1201.
28. Kinnaird, T., E. Stabile, M.S. Burnett, C.W. Lee, S. Barr, S. Fuchs, and S.E. Epstein. 2004. Marrow-derived stromal cells express genes encoding a broad spectrum of arteriogenic cytokines and promote in vitro and in vivo arteriogenesis through paracrine mechanisms. *Circ. Res.* 94:678–685.
29. Laukkanen, M.O., K. Kuramoto, B. Calmels, M. Takatoku, C. von Kalle, R.E. Donahue, and C.E. Dunbar. 2005. Low-dose total body irradiation causes clonal fluctuation of primate hematopoietic stem and progenitor cells. *Blood.* 105:1010–1015.
30. Ponomaryov, T., A. Peled, I. Petit, R.S. Taichman, L. Habler, J. Sandbank, F. Arenzana-Seisdedos, A. Magerus, A. Caruz, N. Fujii, et al. 2000. Induction of the chemokine stromal-derived factor-1 following DNA damage improves human stem cell function. *J. Clin. Invest.* 106: 1331–1339.
31. De Falco, E., D. Porcelli, A.R. Torella, S. Straino, M.G. Iachininoto, A. Orlandi, S. Truffa, P. Biglioli, M. Napolitano, M.C. Capogrossi, et al. 2004. SDF-1 involvement in endothelial phenotype and ischemia-induced recruitment of bone marrow progenitor cells. *Blood.* 104:3472–3482.
32. Kuhel, D.G., B. Zhu, D.P. Witte, and D.Y. Hui. 2002. Distinction in genetic determinants for injury-induced neointimal hyperplasia and diet-induced atherosclerosis in inbred mice. *Arterioscler. Thromb. Vasc. Biol.* 22:955–960.
33. Johnson, C., H.J. Sung, S.M. Lessner, M.E. Fini, and Z.S. Galis. 2004. Matrix metalloproteinase-9 is required for adequate angiogenic revascularization of ischemic tissues: potential role in capillary branching. *Circ. Res.* 94:262–268.
34. Johnson, C., and Z.S. Galis. 2004. Matrix metalloproteinase-2 and -9 differentially regulate smooth muscle cell migration and cell-mediated collagen organization. *Arterioscler. Thromb. Vasc. Biol.* 24:54–60. Epub 2003 Oct 2009.
35. Galis, Z.S., C. Johnson, D. Godin, R. Magid, J.M. Shipley, R.M. Senior, and E. Ivan. 2002. Targeted disruption of the matrix metalloproteinase-9 gene impairs smooth muscle cell migration and geometrical arterial remodeling. *Circ. Res.* 91:852–859.
36. Yee, N.S., I. Paek, and P. Besmer. 1994. Role of kit-ligand in proliferation and suppression of apoptosis in mast cells: basis for radiosensitivity of white spotting and steel mutant mice. *J. Exp. Med.* 179:1777–1787.
37. Rodewald, H.R., M. Dessing, A.M. Dvorak, and S.J. Galli. 1996. Identification of a committed precursor for the mast cell lineage. *Science.* 271:818–822.
38. Fehrenbach, H., M. Haase, M. Kasper, R. Koslowski, D. Schuh, and M. Muller. 1999. Alterations in the immunohistochemical distribution patterns of vascular endothelial growth factor receptors Flk1 and Flt1 in bleomycin-induced rat lung fibrosis. *Virchows Arch.* 435:20–31.
39. Norrby, K. 2002. Mast cells and angiogenesis. *APMIS.* 110:355–371.
40. Grutzkau, A., S. Kruger-Krasagakes, H. Baumeister, C. Schwarz, H. Kogel, P. Welker, U. Lippert, B.M. Henz, and A. Moller. 1998. Synthesis, storage, and release of vascular endothelial growth factor/vascular permeability factor (VEGF/VPF) by human mast cells: implications for the biological significance of VEGF206. *Mol. Biol. Cell.* 9:875–884.
41. Heil, M., and W. Schaper. 2004. Influence of mechanical, cellular, and molecular factors on collateral artery growth (arteriogenesis). *Circ. Res.* 95:449–458.
42. Broudy, V.C. 1997. Stem cell factor and hematopoiesis. *Blood.* 90: 1345–1364.
43. Brown, L.F., K.T. Yeo, B. Berse, T.K. Yeo, D.R. Senger, H.F. Dvorak, and L. van de Water. 1992. Expression of vascular permeability factor (vascular endothelial growth factor) by epidermal keratinocytes during wound healing. *J. Exp. Med.* 176:1375–1379.